Cite this paper as: *Organometallics*, **2016**, *35*, 3221-3226, DOI: acs.organomet.6b00562

Mechanistic investigation of Ir–catalyzed C–H borylation of methyl benzoate: ligand effects in regioselectivity and activity

Jesús Jover,[a,b]* Feliu Maseras,[b,c]*

[a] Departament de Química Inorgànica i Orgànica, Secció de Química Inorgànica, Universitat de Barcelona, Martí i Franquès 1-11, 08028 Barcelona, Spain.

[b] Institute of Chemical Research of Catalonia (ICIQ), The Barcelona Institute of Science and Technology, Avgda. Països Catalans, 16, 43007 Tarragona, Spain.

[c] Departament de Química, Universitat Autònoma de Barcelona, 08193 Bellaterra, Catalonia, Spain.

Supporting Information Placeholder

ABSTRACT: The Ir-catalyzed C–H borylation of methyl benzoate has been studied with DFT methodology in order to understand the experimentally observed ligand-induced regioselectivity and activity when different [(ligand)Ir(Bpin)$_3$] catalysts are employed. While bidentate ligands such as 4,4'-di-^{t}Bu-2,2'-bipyridine (dtbpy) completely inhibit the *ortho*-borylation, the use of selected triphenylphosphine derivatives enables the reaction on that position, avoiding the *meta*- and *para*-regioisomers. The analysis of the catalytic cycles for the borylation reactions with dtbpy, PPh_3, P(*p*-$CF_3C_6H_4)_3$ and P(*m*,*m*-$(CF_3)_2C_6H_3)_3$ allows the interpretation of the observed ligand effects. The different reactivity observed for the different monodentate phosphine ligands can be also rationalized in terms of catalyst stability.

INTRODUCTION

Iridium-catalyzed borylation with bis(pinacolato)diboron (B_2pin_2) or pinacolborane (HBpin) is probably one the best methods to undertake the C–H bond activation and functionalization on organic substrates.[1] One of the most active catalysts to carry out these reactions is $[Ir(OMe)COD]_2$ in combination with bipyridine ligands[2] such as 2,2'-bipyridine or 4,4'-di-^{t}Bu-2,2'-bipyridine (dtbpy) or phenanthroline derivatives.[3] In contrast, the regioselectivity derived from these catalysts is mainly controlled by steric effects and thus, the selective borylation in the *ortho* position of a substituted arene is practically impossible to achieve.[4] In the last years, new methodologies, based on the use of nitrogen,[5] carbonyl[6] and silicon[7] directing groups, have allowed the selective *ortho*-borylation of substituted arenes. Although most procedures employ bidentate nitrogen ligands, other monodentate candidates may also provide good catalysts for the selective *ortho*-borylation of arenes; in 2010 Miyaura *et al.*[6b] reported a catalytic system based on substituted triphenylphosphine ligands that allows the selective *ortho*-borylation of different benzoate esters. Scheme 1 shows the results obtained with different ligands for the borylation of methyl benzoate with the reported iridium-based catalytic system; two ligand effects are observed in the experiments: i) the dtbpy ligand furnishes a very active catalyst but forces the reaction to run under steric control, which means that the pathway yielding the *ortho*-product is completely inhibited; and ii) the triphenylphosphine ligands afford lower yields than dtbpy, but those and the *ortho*-selectivities clearly improve when going from PPh_3 to the more electron-deficient trifluoromethylated versions.

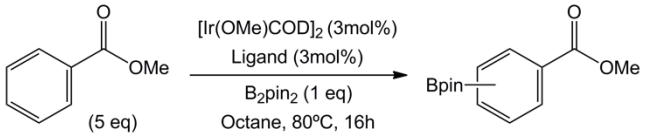

Entry	Ligand	Yield (%)*	*o*-:*m*-:*p*- (%)
1	Dtbpy	145	0:58:42
2	PPh_3	11	64:18:18
3	P(*p*-$CF_3C_6H_4)_3$	45	96:2:2
4	P(*m*,*m*-$(CF_3)_2C_6H_3)_3$	95	98:2:0

Scheme 1. Ir-catalyzed borylation of methyl benzoate (* Yields based on B_2pin_2).

There are therefore two challenging mechanistic aspects that need explanation: the change in selectivity when moving from bipyridine to monophospine, and the yield dependence on the nature of the latter ligand. Herein we report the results obtained in the analysis of the reactions shown in Scheme 1 aiming to understand the observed ligand effects in the Ir-catalyzed borylation of methyl benzoate. Computational chemistry has been already successfully employed in the study of similar boron transition metal chemistry.[4d,8]

COMPUTATIONAL DETAILS

All the structures were fully optimized in 1-octane (PCM, see below) using the Gaussian09 package,[9] with the PBE density functional.[10] The standard 6-31G(d)[11] basis set was used for H, B, C, N, O, F and P atoms; the Stuttgart triple zeta basis set (SDD),[12] along with the associated ECP to describe the 28 core electron, was employed for Ir. Solvation free energies are computed with the (IEF-PCM) continuum dielectric solvation model[13] using the radii and non-electrostatic terms from the SMD solvation model by Truhlar and coworkers.[14] In all cases frequency calculations were carried out to ensure the nature of stationary points and transition states, and to allow the calculation of free energies at 80ºC for all the species involved in the catalytic cycles. Additional single point calculations on the previously optimized geometries were employed to obtain improved solvated free energy values with larger basis sets. The aug-cc-pVTZ-PP basis set including polarization and the associated electron core potential[15] was employed for Ir while the 6-311+G(d,p) basis set[11b] was used for all the other atoms. The solvation model for this additional set of calculations was the same described above. The empirical dispersion terms were computed for the optimized geometries using the DFT-D3 package[16] by Grimme using the corresponding PBE-D3[17] functional. Unless otherwise stated all the free energy values correspond to those obtained with the larger basis set including solvation and dispersion corrections at 80ºC (see SI for details). In order to improve the speed of calculations the ligand dtbpy was simplified to 2,2'-bipyridine and the pinacolatoboron reagents were simplified to the corresponding ethyleneglycolatoboron analogs.

RESULTS AND DISCUSSION

The catalytic cycle of iridium borylations has been proposed and analyzed in various reports.[5a,7a,18] The adaptation to our particular system is shown in Scheme 2. The different coloring for iridium atoms is associated to the oxidation state, black is used for iridium(III) while orange is employed in iridium(V) species. The cycle starts with the iridium(III) species **I**, obtained by reaction of B_2pin_2 and the ligand with the precursor $[Ir(OMe)COD]_2$. The oxidative addition of the C–H bond generates an iridium(V) species **III** that can, in turn, deliver the product by reductive elimination. Finally, the catalyst is regenerated with B_2pin_2 producing HBPin as a side product. Obviously, there are significant nuances in the catalytic cycle depending on the nature of the ligand. Bidentate dtbpy and the monophosphine PPh_3 derivatives favor different numbers of available coordination sites on the metal center, which should have an effect on the selectivity.

First, the computed catalytic cycle for the bidentate ligand dtbpy is described. Table 1 contains the free energy values for all the involved species in the *ortho*-, *meta*- and *para*-borylation reactions with $[(dtbpy)Ir(Bpin)_3]$. Detailed structures, including selected bond distances, of some of these structures are shown in Figure 1. The reaction starts by the coordination of the substrate to the catalyst (**I**) to yield intermediate **II**, where the carboxylate group of the substrate is bound to the metal. The interaction between both moieties is not very strong; this step is slightly endergonic and the distance between the metal and the carbonyl group is as long as 2.63 Å. Although the C–H activation is not possible from this intermediate it serves to bring close the substrate and the catalyst and constitutes the lowest energy isomer of this kind; any other interaction between the metal and the phenyl ring affords higher energy species. Once both counterparts are close enough the decoordination of the CO_2Me group allows the C–H activation to happen. The transition state for this process (**TS_CH**) is lower for the unhindered *meta*- and *para*-positions: 13.0 and 12.4 kcal mol^{-1}, respectively; while 19.4 kcal mol^{-1} are required for the *ortho*-isomer to react. After the C–H activation the pentagonal bipyramid iridium(V) intermediate **III** is obtained, the most stable conformation (linked to the lowest activation transition states) places one Bpin and one nitrogen atom of the ligand in the axial positions, leaving the incoming hydride and phenyl substituents in the equatorial plane. These calculations show, as demonstrated in a previous report,[18b] the late nature of the C–H activation transition states, which display Ir–H distances very similar to those observed in the following complexes **III**. The reaction proceeds by the C–B reductive elimination (**TS_CB**) step. For this to happen both leaving groups have to lie in a *cis* conformation; therefore, the phenyl ring is eliminated along the axial Bpin group, which is the only available option. The barrier from **III** to **TS_CB** is very low and requires less than 2.5 kcal mol^{-1} in all cases.

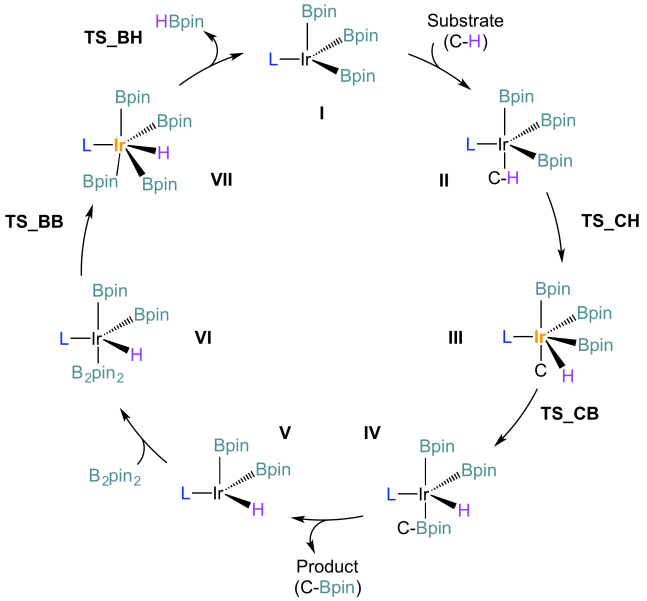

Scheme 2. Catalytic cycle for iridium borylations (Ir(III), Ir(V)).

Table 1. Free energy values (in kcal mol^{-1}) for the *ortho*-, *meta*- and *para*-borylation of methyl benzoate with the [(dtbpy)Ir(Bpin)$_3$] catalyst.

Species	*Ortho*	*meta*	*para*
I	0.0	0.0	0.0
II	5.4	5.4	5.4
TS_CH	24.8	18.4	17.8
III	15.7	8.0	8.1
TS_CB	18.1	9.7	9.6
IV	7.3	5.0	4.5
V	4.0	1.7	1.8
VI	5.2	2.9	3.0
TS_BB	8.1	5.8	5.9
VII	-5.8	-8.1	-8.0
TS_BH	-0.4	-2.7	-2.6
Overall	-4.2	-6.6	-6.4

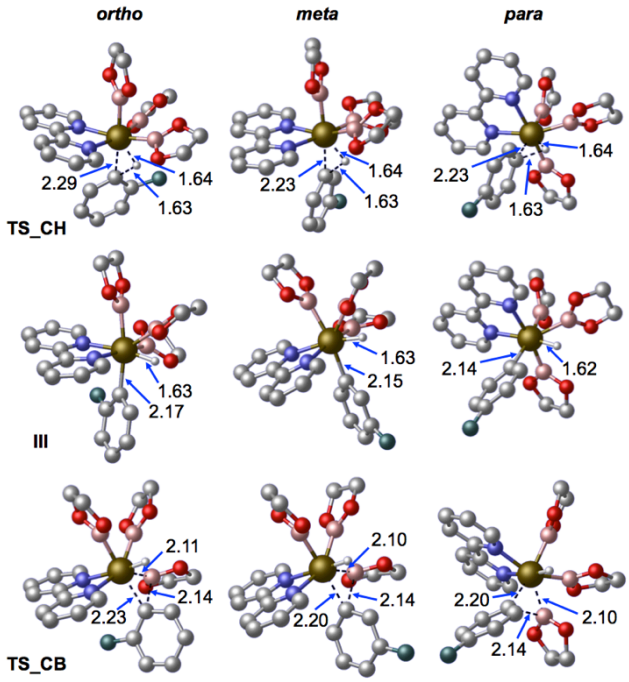

Figure 1. Detailed structures of **TS_CH**, **III** and **TS_CB** for ortho-, meta- and para-borylations with dtbpy. (Distances in Å. Atom color code: C = grey, N = blue, O = red, B = pink, Ir = brown, H = white; for clarity most H atoms have been omitted and the CO_2Me group of the substrate has been replaced by a green ball).

After the reductive elimination, the borylated product remains attached to the metal through the carboxylate (**IV**). The product is then easily released into the reaction mixture to form intermediate **V**, which is always lower in energy than **IV**; this process proceeds by simple diffusion and is probably not mediated by an energy barrier. Once the product is liberated, the pathways for the three isomers converge into complex [(dtbpy)Ir(Bpin)$_2$H] (**V**). From there the catalyst is regenerated by reaction with B_2pin_2; at first, a weak interaction is established between **V** and one of the oxygen atoms of B_2pin_2 to form intermediate **VI**. In this complex, which is 1.3 kcal mol^{-1} higher in energy than **V**, the Ir–O distance is 2.53 Å. Then the B–B activation stage (**TS_BB**), formally an oxidative addition, takes place to deliver the iridium(V) complex **VII**. The transition state mediating this step is clearly asynchronous since both Ir–B distances are quite different: 2.40 vs. 2.55 Å. The barrier for this process (4.1 kcal mol^{-1}) is practically non-existent and, remarkably, the obtained species constitutes the lowest point along the catalytic cycle, making of **VII** the resting state of the studied reaction. The catalytic cycle is closed by the reductive elimination of HBpin (**TS_BH**), which gives back the starting catalyst **I**. This process requires only 5.4 kcal mol^{-1} and thus, this stage is expected to be very fast. Detailed structures of **VI**, **TS_BB**, **VII** and **TS_BH**, including selected bond distances, can be found in Figure 2. The overall thermodynamics indicate that the studied reactions are exergonic by 4.2, 6.6 and 6.4 kcal mol^{-1} for the *ortho*-, *meta*- and *para*-borylated products, respectively.

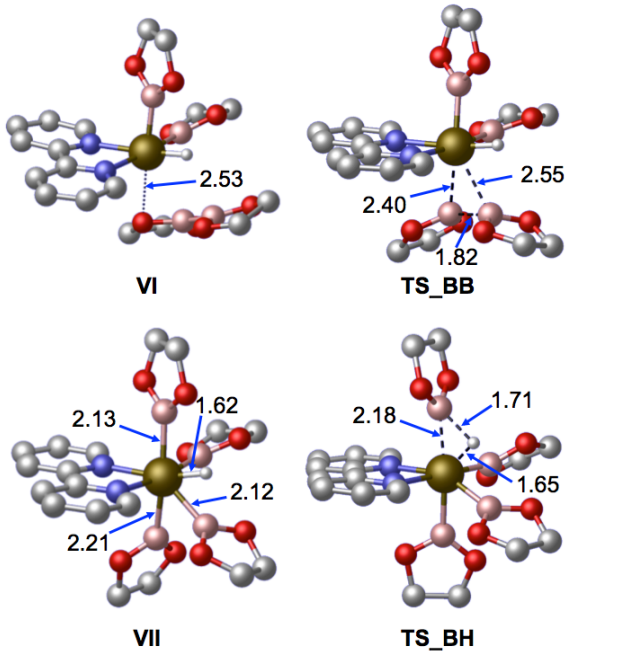

Figure 2. Detailed structures of **VI**, **TS_BB**, **VII** and **TS_BH** for methyl benzoate borylation with dtbpy. (Distances in Å. Atom color code: C = grey, N = blue, O = red, B = pink, Ir = brown, H = white; for clarity most H atoms have been omitted).

The computed free energies allow the calculation of the apparent activation energy for the reaction, which can be related to the turnover frequency. This is done applying the energetic span model developed by Kozuch and Shaik.[19] This methodology states that the apparent activation barrier corresponds to the reaction energy plus the energy difference between the highest and the lowest species when the former appears first in the catalytic cycle, as in this study. Thus, the apparent activation barriers for the *ortho*-, *meta*- and *para*-borylation reactions, computed as the free energy difference between **VII** and **TS_CH** plus the overall reaction free energy, are 26.4, 19.9 and 19.4 kcal mol^{-1}, respectively. These values agree with the experimental observation that the borylation product mixture does not contain any *ortho*-regioisomer; moreover, the barrier for the *meta*-derivative is slightly higher than that for the *para*-

borylated product, in agreement with the observed experimental 1:1.45 (per site) ratio. The origin of the higher free energy for **TS_CH** in the case of the *ortho*-regioisomer can be readily associated to the steric repulsion between the CO_2Me group and the rest of the system. It is obvious from the structures in Figure 1 that in this isomer, the carboxylate group is much closer to the already crowded metal center. The preference of the system with the dtbpy ligand for the *meta*- and *para*-borylation products is thus explained.

The catalytic cycle was recomputed for the three triphenylphosphine ligand derivatives. We decided to use only one phosphine instead of two in our computational model because this corresponds to the stoichiometry used in the experimental study. For the sake of completion, we computed also the three hypothetical diphosphine complexes, and found that the binding of a second phosphine to the monophosphine system is indeed exergonic by 17.2, 21.3 and 27.6 kcal mol^{-1} for PPh_3, P(*p*-$CF_3C_6H_4)_3$ and P(*m*,*m*-$(CF_3)_2C_6H_3)_3$, respectively. However, the equilibrium between two $(PR_3)Ir(Bpin)_3$ complexes and $(PR_3)_2Ir(Bpin)_3$ plus $Ir(BPin)_3$ is clearly

Table 2. Free energy values (in kcal mol^{-1}) for the *ortho*-, *meta*- and *para*-borylation of methyl benzoate with triphenylphosphine ligands.

	PPh_3			**P(*p*-$CF_3C_6H_4)_3$**			**P(*m*,*m*-$(CF_3)_2C_6H_3)_3$**		
Species	***ortho***	***Meta***	***para***	***ortho***	***meta***	***para***	***ortho***	***Meta***	***para***
I	0.0	0.0	0.0	0.0	0.0	0.0	0.0	0.0	0.0
II	3.2	3.2	3.2	-0.2	-0.2	-0.2	2.6	2.6	2.6
TS_CH	10.8	18.4	18.4	8.1	16.8	16.9	16.4	19.9	21.0
III	4.2	12.2	11.5	3.9	12.9	9.9	10.0	12.9	14.6
TS_CB	16.1	18.7	20.1	13.8	19.2	17.8	20.0	22.2	20.9
IV	5.4	2.4	2.8	3.0	-0.3	0.8	5.0	9.8	1.3
V	1.1	-1.3	-1.1	1.3	-1.0	-0.9	2.1	-0.2	-0.1
VI	1.4	-1.0	-0.8	1.0	-1.3	-1.2	8.2	5.9	6.0
TS_BB	11.4	9.0	9.2	8.6	6.3	6.4	10.8	8.5	8.6
VII	-5.5	-7.9	-7.7	-7.2	-9.5	-9.4	-4.7	-7.0	-6.9
TS_BH	-2.6	-5.0	-4.8	-5.5	-7.8	-7.7	-1.5	-3.8	-3.7
Overall	-4.2	-6.6	-6.4	-4.2	-6.6	-6.4	-4.2	-6.6	-6.4

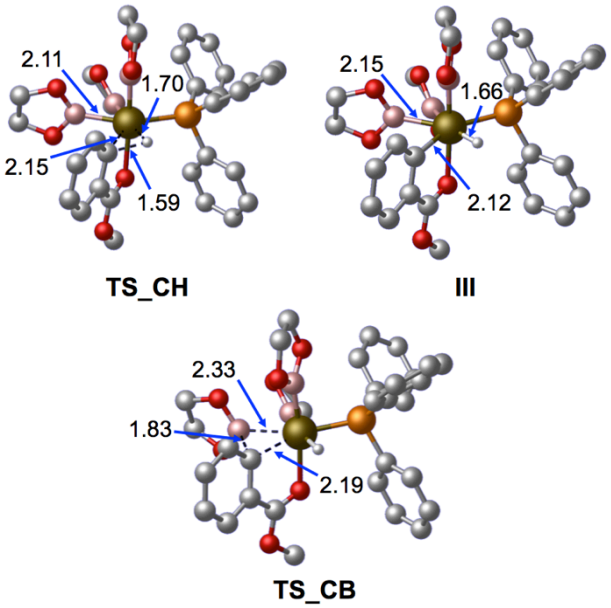

Figure 3. Detailed structures of **TS_CH**, **III** and **TS_CB** for the *ortho*-borylation of methyl benzoate with the Ir/PPh_3 catalyst. (Distances in Å. Atom color code: C = grey, P =orange, O = red, B = pink, Ir = brown, H = white; for clarity most H atoms have been omitted).

displaced towards the former by 13.6, 9.9 and 20.4 kcal mol^{-1} for PPh_3, P(*p*-$CF_3C_6H_4)_3$ and P(*m*,*m*-$(CF_3)_2C_6H_3)_3$, thus confirming that the monophosphine complexes should be predominant under the experimental conditions. The relative free energy profiles for the *ortho*-, *meta*- and *para*-borylation reactions with the tri-phenylphosphine ligand derivatives can be found in Table 2. The main qualitative difference with the results reported above is that only one monophosphine ligand coordinates iridium. The obtained geometries for all the systems are very similar; as an example, detailed structures of **TS_CH**, **III** and **TS_CB** with PPh_3 ligand are shown in Figure 3. As above, the reaction starts by the coordination of the substrate through the carboxylate group to the active iridium catalyst to form intermediate **II**. This step is slightly exergonic for P(*p*-$CF_3C_6H_4)_3$ probably due to the electron-withdrawing character of the trifluoromethyl group on the phenyl rings. In the case of P(*m*,*m*-$(CF_3)_2C_6H_3)_3$, which is a stronger electron acceptor, this stage turns out to be endergonic by 2.6 kcal mol^{-1}. This behavior could be attributed to the larger steric congestion induced by the ligand on the iridium coordination sphere after the substrate coordination. Once **II** is obtained the reaction proceeds by the C–H activation (**TS_CH**), following either the *ortho*-directed borylation pathway or the undirected C–H activation pathways leading to the *meta*- or *para*-borylation products; these options are likely to imply the substrate dissociation prior to the C–H activation. As may be observed the directed C–H_{ortho} activation is always the favored one for the three ligands employed. In the case of PPh_3,

TS_CH$_{ortho}$ is almost 8 kcal mol^{-1} lower than the other C–H activation pathways (10.8, 18.4 and 18.4 kcal mol^{-1}, for the C–H activation in *ortho*-, *meta*- and *para*-positions, respectively). The same trend is observed with P(*p*-$CF_3C_6H_4)_3$ and P(*m*,*m*-$(CF_3)_2C_6H_3)_3$, although the energy difference between the three **TS_CH** transition states obtained with the latter ligand is slightly smaller. This could be attributed again to the larger steric hindrance induced by this ligand on the iridium(V) complexes. The **TS_CH$_{ortho}$** barriers follow the expected trend and correlate with the electron-donating ability and the sterics of the ligands *i.e.* values of 7.6, 8.3 and 13.8 kcal mol^{-1} for PPh_3, P(*p*-$CF_3C_6H_4)_3$ and P(*m*,*m*-$(CF_3)_2C_6H_3)_3$, respectively. PPh_3 is the smallest and the most-electron donating ligand, and has the lowest barrier whereas P(*m*,*m*-$(CF_3)_2C_6H_3)_3$, the largest and more electron-demanding ligand, has the highest barrier. After the C–H activation, intermediate **III** is formed. In the case of the C–H$_{ortho}$ activation these complexes are lower in energy because the carboxylate group acts as a ligand, and completes the coordination sphere of the iridium(V) center. In all the **III$_{ortho}$** species the iridium atom adopts a pentagonal bipyramid structure with the carboxylate and one Bpin group occupying the axial positions. This leaves the phenyl group situated between the hydride and one Bpin group in the equatorial plane, in a perfect arrangement for the reaction to proceed by elimination of the C–B bond. A similar coordination sphere is obtained for complexes **III$_{meta}$** and **III$_{para}$** although in these cases the iridium atom adopts a pentagonal pyramid structure, with one of the Bpin substituents in the axial position. The octahedral analogues for these latter intermediates have been found to lie at higher energies, probably due to the strong trans influence of all the substituents on the metal: a hydride, a phosphine, a phenyl ring and three Bpin groups. This effect is probably minimized in the pentagonal pyramid structure, where the substituents do not face another one in a direct trans conformation. The reaction proceeds by jumping over the reductive elimination barrier.

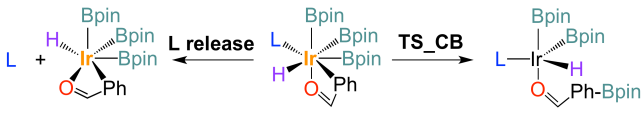

III' **III** **IV**

Ligand (L)	III	TS_CB	III'
PPh_3	0.0	11.9	10.1
P(*p*-$CF_3C_6H_4)_3$	0.0	9.9	10.8
P(*m*,*m*-$(CF_3)_2C_6H_3)_3$	0.0	10.0	21.4

Scheme 3. Competing ligand release vs. C–B elimination from intermediate III, relative free energies are given in kcal mol^{-1} (Ir(III), Ir(V)).

The corresponding **TS_CB** transition state mediates this process and is, in all cases, the highest energy point along the reaction coordinate. Among all the possible **TS_CB** barriers, the most favored are always those leading to the *ortho*-borylated products; which are, indeed, the major products observed experimentally. These results clearly indicate that the *ortho*-directed pathway is always the preferred one when employing monodentate phosphine ligands. After the reductive elimination the product is liberated and the initial catalyst is recovered by reaction with B_2pin_2 (*i.e.*, from **V** to **VII**, Scheme 1). The barriers obtained in this last part of the cycle are relatively low, usually below 10 kcal mol^{-1}. As before, complex **VII** [(PR_3)Ir$(Bpin)_4$H] has the lowest relative free energy along the reaction pathway and is the resting state of the overall reaction. The preference of the monophosphine systems for ortho-borylation is then satisfactorily reproduced by calculation. In contrast to the bipyridine ligand, the oxygen can coordinate in this case to iridium, and thus drive the reaction towards the closest C–H bond. The results reported above provide a justification to why the monophosphine systems favor *ortho*- *vs meta*- or *para*-borylation, but they do not provide any explanation to the substantial differences in yield associated to the different monophosphine systems. Indeed, the apparent reaction barriers for the *ortho*-borylation of methyl benzoate, computed as the free energy difference between **VII** and **TS_CB** plus the overall reaction energy, are 17.4, 16.8 and 20.5 kcal mol^{-1} for the catalysts containing PPh_3, P(*p*-$CF_3C_6H_4)_3$ and P(*m*,*m*-$(CF_3)_2C_6H_3)_3$, respectively. These results do not match the observed reactivity and indicate that, under the experimental conditions, all the three ligand may furnish very good catalysts, with P(*p*-$CF_3C_6H_4)_3$ as the best choice. In addition, the regioselectivity observed for PPh_3 (64:18:18) cannot be explained with the computed free energy profile, which indicates an absolute dominance of the *ortho*-borylated product. We think that the explanation to the different yields obtained is associated to the stability of species **III**; this iridium(V) intermediate is sterically crowded and an alternative mechanism could dissociate the phosphine ligand, giving rise to the iridium(V) complex **III'**, instead of reductively eliminating the borylated product (Scheme 3). If the role of **III'** was only to be in equilibrium with **III**, it would not affect the reaction outcome, as its concentration should be negligible with respect to that of **III** because of the free energy difference. But we postulate that **III'**, without the phosphine ligand is likely to evolve into an unreactive species, either through precipitation or through entry of other blocking ligands. This hypothesis has some experimental support. It has been stated that the borylation reaction without any ligand is slow (13% yield) and gives no selectivity at all (38:38:24). We can also support this hypothesis with calculations: for PPh_3 the ligand loss is indeed effectively competing with the catalytic borylation; this process is energetically favored over the C–B reductive elimination and thus it could eventually lead to the depletion of the active species. When the PPh_3 ligand is lost, likely after a few turnovers, the reaction enters in a completely different regime and the initially obtained *ortho*-selectivity starts to fade away. This might also happen to the catalyst with P(*p*-$CF_3C_6H_4)_3$, although in this case the ligand loss should be less pronounced. In addition, the liberated phosphine ligand could irreversibly coordinate to other iridium(III) species such as **I** or **V** to deliver the [$(PR_3)_2$Ir$(Bpin)_3$] or [$(PR_3)_2$Ir$(Bpin)_2$H] intermediates, which are likely inactive. Thus, for each ligand released two catalyst molecules would become inactive. The coordination of both PPh_3 and P(*p*-$CF_3C_6H_4)_3$ to their corresponding complex **I** has been found to be exergonic by almost 20 kcal mol^{-1}, indicating that once the bisligated iridium complex is formed, it is practically impossible to go back to the active monoligated version of the catalyst. These results are consistent with the low activity of the catalyst bearing the PPh_3 ligand and its regioselectivity pattern. In the case of P(*p*-$CF_3C_6H_4)_3$ the catalyst seems to remain stable for a longer period, allowing an enhanced activity and selectivity. In contrast, for P(*m*,*m*-$(CF_3)_2C_6H_3)_3$ the energy difference between the ligand loss and reductive elimination from **III** clearly favors the C–B elimination over the ligand dissociation; there-

fore, the catalytic system carrying this ligand produces the most active and selective phosphine-based borylation platform for methyl benzoate.

A last point deserving comment is the presence of yields above 100% in Table 1, taken from experimental work. In particular, the B_2Pin_2-based yield for the system with the dtbpy ligand is 145%. This means that not one, but two BPin units are transferred from the same B_2Pin_2 molecule. The HBpin product from the reaction studied here must also react with the substrate. We suspect that the mechanism may be similar, but we did not study it because it is out of the scope of this work. In a related topic, we cannot predict from the available data if HBPin is reactive in the systems with a monophosphine ligand. It may be that the yield below 100% is related to a lack of reactivity of HBPin, or to an overall lower reactivity of both B_2Pin_2 and HBPin. Again, this aspect concerning HBPin reactivity is out of the scope of this work.

CONCLUSIONS

The Ir-catalyzed C–H borylation of methyl benzoate has been successfully studied by computational means for systems using the bidentate ligand dtbpy and the monodentate phosphine ligands PPh_3, P(*p*-$CF_3C_6H_4)_3$ and P(*m*,*m*-$(CF_3)_2C_6H_3)_3$. The ligand effects responsible of the observed regioselectivity obtained for those systems have been studied

When the bidentate ligand dtbpy is employed the borylation reaction is under steric control and thus the *ortho*-borylation pathway is completely shut down. Conversely, the *meta*- and *para*-borylation reactions are quite fast but the process is non-selective since the activation barriers are quite close.

In the case of the monodentate phosphine ligands the selective *ortho*-borylation reaction is shown to be clearly favored over the undirected *meta*- and *para*-borylation of methyl benzoate because of the directing effect of the carbonyl group which in this case can coordinate the metal. Finally, the computations also provide an explanation for the observed reactivity between phosphines; the stability of the iridium(V) intermediates towards ligand dissociation plays a crucial role in the reaction, since PPh_3 and P(*p*-$CF_3C_6H_4)_3$ show higher ligand lability and make worse catalysts than P(*m*,*m*-$(CF_3)_2C_6H_3)_3$.

ASSOCIATED CONTENT

Supporting Information

DFT computed energies and dispersion terms. The supplemental file "geometries.xyz" contains the computed Cartesian coordinates of all of the molecules reported in this study. The file may be opened as a text file to read the coordinates, or opened directly by a molecular modeling program such as Mercury (version 3.3 or later, http://www.ccdc.cam.ac.uk/pages/Home.aspx) for visualization and analysis. The Supporting Information is available free of charge on the ACS Publications website.

AUTHOR INFORMATION

Corresponding Author

* Feliu Maseras, *e*-mail: fmaseras@iciq.es
* Jesús Jover, *e*-mail: jesus.jover@qi.ub.es

Notes

The authors declare no competing financial interest.

ACKNOWLEDGMENT

The ICIQ Foundation and the Spanish Government Grant CTQ2014-57761-R supported this work. J.J. thanks the Government of Spain (MINECO) for a Juan de la Cierva Fellowship (JCI-2011-10134).

REFERENCES

(1) (a) Cho, J.-Y.; Tse, M. K.; Holmes, D.; Maleczka, R. E.; Smith, M. R. *Science* **2002**, 295, 305-308; (b) Mkhalid, I. A. I.; Barnard, J. H.; Marder, T. B.; Murphy, J. M.; Hartwig, J. F. *Chem. Rev.* **2010**, 110, 890-931; (c) Choi, J.; Goldman, A. S., Iridium Catalysis. In *Ir-catalyzed functionalization of C-H bonds*, Andersson, P. G., Ed. Springer-Verlag: Berlin, 2011; Vol. 34, pp 139-167; (d) Ros, A.; Fernandez, R.; Lassaletta, J. M. *Chem. Soc. Rev.* **2014**, 43, 3229-3243.

(2) (a) Ishiyama, T.; Takagi, J.; Hartwig, J. F.; Miyaura, N. *Angew. Chem. Int. Ed.* **2002**, 41, 3056-3058; (b) Crawford, A. G.; Liu, Z.; Mkhalid, I. A. I.; Thibault, M.-H.; Schwarz, N.; Alcaraz, G.; Steffen, A.; Collings, J. C.; Batsanov, A. S.; Howard, J. A. K.; Marder, T. B. *Chem. Eur. J.* **2012**, 18, 5022-5035; (c) Lee, C.-I.; Shih, W.-C.; Zhou, J.; Reibenspies, J. H.; Ozerov, O. V. *Angew. Chem. Int. Ed.* **2015**, 54, 14003-14007; (d) Sasaki, I.; Taguchi, J.; Doi, H.; Ito, H.; Ishiyama, T. *Chem. Asian J.* **2016**, 11, 1400-1405.

(3) (a) Ishiyama, T.; Takagi, J.; Ishida, K.; Miyaura, N.; Anastasi, N. R.; Hartwig, J. F. *J. Am. Chem. Soc.* **2002**, 124, 390-391; (b) Liskey, C. W.; Hartwig, J. F. *J. Am. Chem. Soc.* **2013**, 135, 3375-3378; (c) Larsen, M. A.; Hartwig, J. F. *J. Am. Chem. Soc.* **2014**, 136, 4287-4299.

(4) (a) Hurst, T. E.; Macklin, T. K.; Becker, M.; Hartmann, E.; Kügel, W.; Parisienne-La Salle, J.-C.; Batsanov, A. S.; Marder, T. B.; Snieckus, V. *Chem. Eur. J.* **2010**, 16, 8155-8161; (b) Hartwig, J. F. *Chem. Soc. Rev.* **2011**, 40, 1992-2002; (c) Hartwig, J. F. *Acc. Chem. Res.* **2012**, 45, 864-873; (d) Tajuddin, H.; Harrisson, P.; Bitterlich, B.; Collings, J. C.; Sim, N.; Batsanov, A. S.; Cheung, M. S.; Kawamorita, S.; Maxwell, A. C.; Shukla, L.; Morris, J.; Lin, Z.; Marder, T. B.; Steel, P. G. *Chem. Sci.* **2012**, 3, 3505-3515; (e) Robbins, D. W.; Hartwig, J. F. *Angew. Chem. Int. Ed.* **2013**, 52, 933-937; (f) Larsen, M. A.; Wilson, C. V.; Hartwig, J. F. *J. Am. Chem. Soc.* **2015**, 137, 8633-8643.

(5) (a) Ros, A.; Estepa, B.; López-Rodríguez, R.; Álvarez, E.; Fernández, R.; Lassaletta, J. M. *Angew. Chem. Int. Ed.* **2011**, 50, 11724-11728; (b) López-Rodríguez, R.; Ros, A.; Fernández, R.; Lassaletta, J. M. *J. Org. Chem.* **2012**, 77, 9915-9920; (c) Roering, A. J.; Hale, L. V. A.; Squier, P. A.; Ringgold, M. A.; Wiederspan, E. R.; Clark, T. B. *Org. Lett.* **2012**, 14, 3558-3561; (d) Roosen, P. C.; Kallepalli, V. A.; Chattopadhyay, B.; Singleton, D. A.; Maleczka, R. E.; Smith, M. R. *J. Am. Chem. Soc.* **2012**, 134, 11350-11353; (e) Ros, A.; López-Rodríguez, R.; Estepa, B.; Álvarez, E.; Fernández, R.; Lassaletta, J. M. *J. Am. Chem. Soc.* **2012**, 134, 4573-4576; (f) Bisht, R.; Chattopadhyay, B. *J. Am. Chem. Soc.* **2016**, 138, 84-87.

(6) (a) Kawamorita, S.; Ohmiya, H.; Hara, K.; Fukuoka, A.; Sawamura, M. *J. Am. Chem. Soc.* **2009**, 131, 5058-5059; (b) Ishiyama, T.; Isou, H.; Kikuchi, T.; Miyaura, N. *Chem. Comm.* **2010**, 46, 159-161; (c) Kawamorita, S.; Ohmiya, H.; Sawamura, M. *J. Org. Chem.* **2010**, 75, 3855-3858; (d) Yamazaki, K.; Kawamorita, S.; Ohmiya, H.; Sawamura, M. *Org. Lett.* **2010**, 12, 3978-3981.

(7) (a) Boebel, T. A.; Hartwig, J. F. *J. Am. Chem. Soc.* **2008**, 130, 7534-7535; (b) Larsen, M. A.; Cho, S. H.; Hartwig, J. *J. Am. Chem. Soc.* **2016**, 138, 762-765.

(8) (a) Kleeberg, C.; Dang, L.; Lin, Z.; Marder, T. B. *Angew. Chem. Int. Ed.* **2009**, 48, 5350-5354; (b) Pubill-Ulldemolins, C.; Poyatos, M.; Bo, C.; Fernandez, E. *Dalton Trans.* **2013**, 42, 746-752; (c) Cheung, M. S.; Sheong, F. K.; Marder, T. B.; Lin, Z. *Chem. Eur. J.* **2015**, 21, 7480-7488.

(9) Frisch, M. J.; Trucks, G. W.; Schlegel, H. B.; Scuseria, G. E.; Robb, M. A.; Cheeseman, J. R.; Scalmani, G.; Barone, V.; Mennucci,

B.; Petersson, G. A.; Nakatsuji, H.; Caricato, M.; Li, X.; Hratchian, H. P.; Izmaylov, A. F.; Bloino, J.; Zheng, G.; Sonnenberg, J. L.; Hada, M.; Ehara, M.; Toyota, K.; Fukuda, R.; Hasegawa, J.; Ishida, M.; Nakajima, T.; Honda, Y.; Kitao, O.; Nakai, H.; Vreven, T.; Montgomery, J., J. A.; Peralta, J. E.; Ogliaro, F.; Bearpark, M.; Heyd, J. J.; Brothers, E.; Kudin, K. N.; Staroverov, V. N.; Kobayashi, R.; Normand, J.; Raghavachari, K.; Rendell, A.; Burant, J. C.; Iyengar, S. S.; Tomasi, J.; Cossi, M.; Rega, N.; Millam, N. J.; Klene, M.; Knox, J. E.; Cross, J. B.; Bakken, V.; Adamo, C.; Jaramillo, J.; Gomperts, R.; Stratmann, R. E.; Yazyev, O.; Austin, A. J.; Cammi, R.; Pomelli, C.; Ochterski, J. W.; Martin, R. L.; Morokuma, K.; Zakrzewski, V. G.; Voth, G. A.; Salvador, P.; Dannenberg, J. J.; Dapprich, S.; Daniels, A. D.; Farkas, Ö.; Foresman, J. B.; Ortiz, J. V.; Cioslowski, J. F., D. J. *Gaussian09, Revision A.02*, Gaussian, Inc.: Wallingford CT, **2009**.

(10) (a) Perdew, J. P.; Burke, K.; Ernzerhof, M. *Phys. Rev. Lett.* **1996**, 77, 3865; (b) Perdew, J. P.; Burke, K.; Ernzerhof, M. *Phys. Rev. Lett.* **1997**, 78, 1396.

(11) (a) Hariharan, P. C.; Pople, J. A. *Theor. Chem. Acc.* **1973**, 28, 213-222; (b) Frisch, M. J.; Pople, J. A.; Binkley, J. S. *J. Chem. Phys.* **1984**, 80, 3265-3269.

(12) (a) Dunning, T. H.; Hay, P. J., In *Modern Theoretical Chemistry*, Schaefer III, H. F., Ed. Plenum: New York, 1976; Vol. 3, pp 1-28; (b) Bergner, A.; Dolg, M.; Küchle, W.; Stoll, H.; Preuss, H. *Molecular Physics* **1993**, 80, 1431 - 1441.

(13) (a) Tannor, D. J.; Marten, B.; Murphy, R.; Friesner, R. A.; Sitkoff, D.; Nicholls, A.; Honig, B.; Ringnalda, M.; Goddard, W. A. *J. Am. Chem. Soc.* **1994**, 116, 11875-11882; (b) Marten, B.; Kim, K.; Cortis, C.; Friesner, R. A.; Murphy, R. B.; Ringnalda, M. N.; Sitkoff, D.; Honig, B. *J. Phys. Chem.* **1996**, 100, 11775-11788.

(14) Marenich, A. V.; Cramer, C. J.; Truhlar, D. G. *J. Phys. Chem. B* **2009**, 113, 6378-6396.

(15) Figgen, D.; Peterson, K. A.; Dolg, M.; Stoll, H. *J. Chem. Phys.* **2009**, 130, 164108-164112.

(16) *DFT-D3 A dispersion correction for density functionals, Hartree-Fock and semi-empirical quantum chemical methods*, 2.1 Rev. 3; Universität Bonn: **2011**.

(17) (a) Grimme, S. *J. Comput. Chem.* **2004**, 25, 1463-1473; (b) Grimme, S. *J. Comput. Chem.* **2006**, 27, 1787-1799; (c) Grimme, S. *J. Chem. Phys.* **2010**, 132, 154104.

(18) (a) Tamura, H.; Yamazaki, H.; Sato, H.; Sakaki, S. *J. Am. Chem. Soc.* **2003**, 125, 16114-16126; (b) Green, A. G.; Liu, P.; Merlic, C. A.; Houk, K. N. *J. Am. Chem. Soc.* **2014**, 136, 4575-4583; (c) Huang, G.; Kalek, M.; Liao, R.-Z.; Himo, F. *Chem. Sci.* **2015**, 6, 1735-1746; (d) Santoro, S.; Kalek, M.; Huang, G.; Himo, F. *Acc. Chem. Res.* **2016**, 49, 1006-1018.

(19) Kozuch, S.; Shaik, S. *Acc. Chem. Res.* **2010**, 44, 101-110.

TABLE OF CONTENTS GRAPHIC